

Supplementary Information.

Panchromatic Triple Organic Semiconductor Heterojunctions for Efficient Solar Cells.

*Cristina Rodríguez-Seco¹, Lydia Cabau¹, Maria Privado², Pilar de la Cruz², Fernando Langa^{*2}, Ganesh D. Sharma^{*3}, Emilio Palomares^{1,4*}*

1. Institute of Chemical Research of Catalonia-The Barcelona Institute of Science and Technology (ICIQ-BIST). Avda. Països Catalans, 16. Tarragona. E-43007. Spain.
2. Universidad de Castilla-La Mancha, Institute of Nanoscience, Nanotechnology and Molecular Materials (INAMOL), Campus de la Fábrica de Armas, 45071-Toledo, Spain
3. Department of Physics, The LNM Institute of Information Technology (Deemed University), Rupa ki Nagal, Jamdoli, Jaipur, India
4. ICREA. Passeig Lluís Companys, 23. Barcelona. E-08010. Spain

Fernando Langa: fernando.langa@uclm.es

Ganesh D. Sharma: gdsharma273@gmail.com

Emilio Palomares: epalomares@icq.es

EXPERIMENTAL

Device fabrication and characterization

Indium tin oxide (ITO) coated glass substrates with a sheet resistance of 10-12 $\Omega \text{ cm}^{-2}$ were thoroughly cleaned prior to device fabrication by soaking in detergent solution followed by ultrasonication in deionized water, acetone and isopropyl alcohol sequentially for 15 min. The substrates were dried in vacuum overnight and a 40 nm thick poly(styrenesulfonate)-doped poly(3,4-ethylenedioxythiophene) (PEDOT:PSS) (Bayer Baytron 4083) layer was spin-coated on the ITO-coated glass substrates at 2500 rpm for 30 s. The substrates were dried at 110 °C for 10 min in under air conditions. The active layers were spun from solutions of LCS01 or EP02:PC₇₁BM at different weight ratios of 1:1, 1:1.5, 1:2 and 1:2.5 with an overall concentration of 14 mg/mL from chloroform. Solvent vapor annealing (SVA) of active layers spin coated from solution in a blend of CF with weight ratio of 1:2 was carried out by placing the substrate in a glass petri dish containing 0.3 mL THF for 40 s. On top of the active layer, a thin PFN layer was spin coated at a concentration of 1.5 mg/mL on at 3000 rpm for 30 s. Finally, the aluminum (Al) top electrode was thermally deposited on the top in a vacuum of 10^{-5} Torr through a shadow mask area of 20 mm². All devices were fabricated and tested in an ambient atmosphere without encapsulation. The hole-only devices with architectures of ITO/PEDOT:PSS/active layer/Au were also fabricated in a similar way in order to measure the hole mobility. The current-voltage (J-V) characteristics of the BHJ organic solar cells were measured using a computer-controlled Keithley 2400 source meter in the dark and under simulated AM1.5G illumination of 100 mW/cm². A xenon light source coupled with an optical filter was used to provide stimulated irradiance at the surface of

the devices. The incident photon-to-current efficiency (IPCE) of the devices was measured by Benthem IPCE system.

Table S1. Optical and electrochemical values for the electron donor and electron acceptor molecules.

Molecule	$\lambda_{\max, \text{abs}}$ (nm) ^[a]	ϵ (M ⁻¹ cm ⁻¹)	$\lambda_{\max, \text{em}}$ (nm) ^[a]	E_{0-0} (eV)	HOMO [eV] ^[b]	LUMO [eV] ^[b]
EP02	460	2.7 x 10 ⁴	621	2.34	-5.36	-3.02
LCS01	473	3.8 x 10 ⁴	669	2.23	-5.16	-2.93
MPU3	628	3.4 x 10 ⁴	730	1.52	-5.61	-3.74

[a] In dichloromethane solution; [b] Obtained from CV, measured in dichloromethane and using Fc/Fc⁺ as internal reference.

Table S2 Photovoltaic parameters of ternary **EP02:PC₇₁BM:MPU3** based OSCs with different weight ratios of PC₇₁BM and MPU3

EP02:PC₇₁BM:MPU3	J_{sc} (mA/cm ²)	V_{oc} (V)	FF	PCE (%)
1:0.2:1.3	11.35	0.97	0.49	5.39
1:0.4:1.1	12.98	0.97	0.51	6.42
1:0.5:1.0	13.39	0.98	0.52	6.82
1:0.6:0.9	12.86	0.96	0.50	6.17

Table S3 Photovoltaic parameters of ternary **LCS01:PC₇₁BM:MPU3** based OSCs with different weight ratios of PC₇₁BM and MPU3

LCS01:PC₇₁BM:MPU3	J_{sc} (mA/cm ²)	V_{oc} (V)	FF	PCE (%)
1:0.2:1.3	11.73	0.87	0.51	5.20
1:0.4:1.1	13.45	0.86	0.53	6.13
1:0.5:1.0	13.91	0.86	0.55	6.58
1:0.6:0.9	13.12	0.84	0.53	5.84

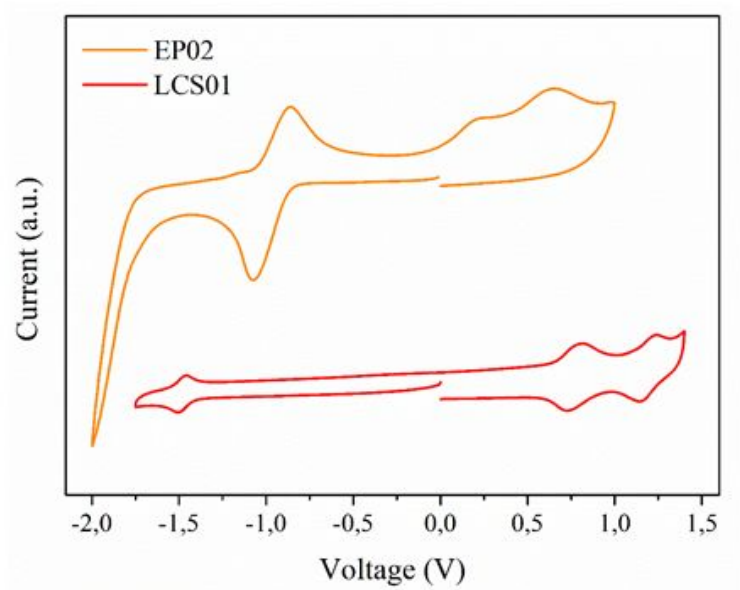


Figure S1: Cyclic voltammetry of EP02 and LCS01 measured using ferrocene as an internal reference at room temperature with a scan rate of 10 mV/s.

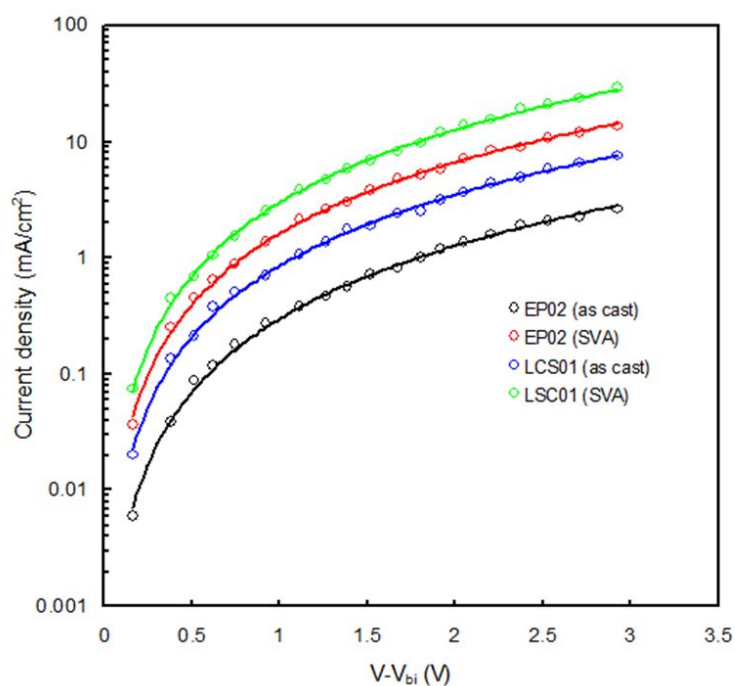


Figure S2. Dark current –voltage characteristics of hole only devices using as cast and SVA treated LCS01:PC₇₁BM and EP02:PC₇₁BM active layers. Solid lines are SCLC fitting to the Equation 1S.

$$J_{\text{SCLC}} = (9/8) \epsilon_0 \epsilon_r \mu [(V - V_{\text{bi}})^2 / d^3] \text{-----Equation S1}$$

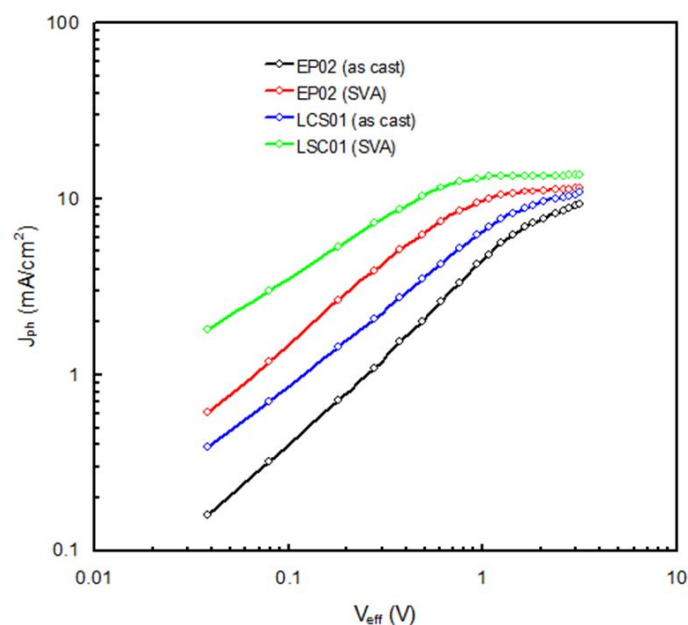


Figure S3. Variation of photocurrent density (J_{ph}) with effective voltage (V_{eff}) for OSCs based on as cast and SVA treated LCS01:PC₇₁BM and EP02:PC₇₁BM active layers.

X-ray diffraction characterization

The SMs showed high crystallinity as confirmed from the X-ray diffraction (XRD) measurements (**Figure 4S**). Both the SMs exhibit same (100) diffraction peak located at $2\theta = 4.92$ corresponding to the same lamellar distance of 1.93 nm. However, the (010) diffraction peak, arises from the π - π stacking is located at $2\theta = 21.54$ and 22.16 for EP02 and LCS01, respectively, corresponds to the π - π distance of 3.95 and 3.87, respectively. Moreover, the intensity of diffraction peaks for LCS01 is higher than EP02, indicating LCS01 exhibits higher crystallinity than EP02. From this data we expect that the higher crystallinity and compact π - π stacking distance of LCS01 leads to higher hole mobility.

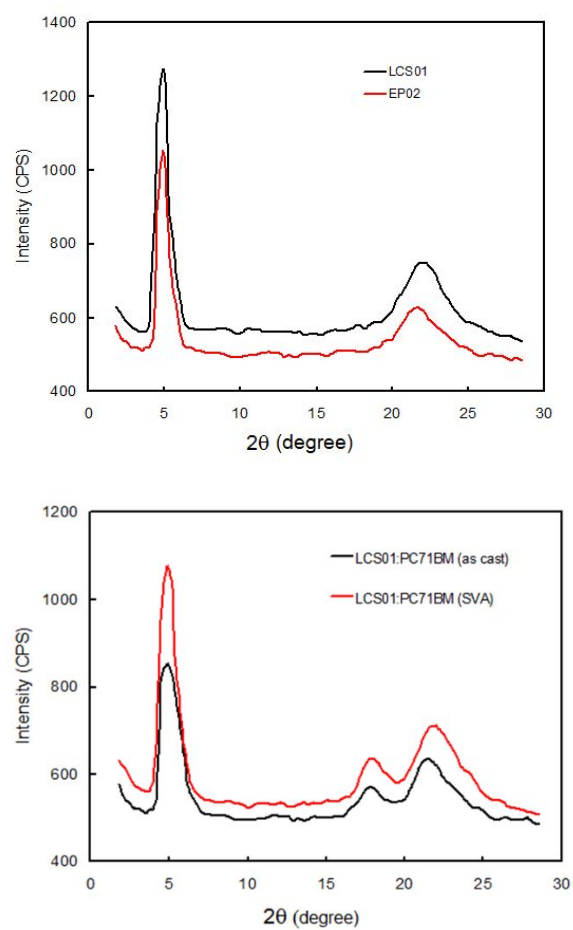


Figure S4. The XRD patterns of LCS01 and EP02 thin films (top) and LCS01:PC₇₁BM thin films (bottom)

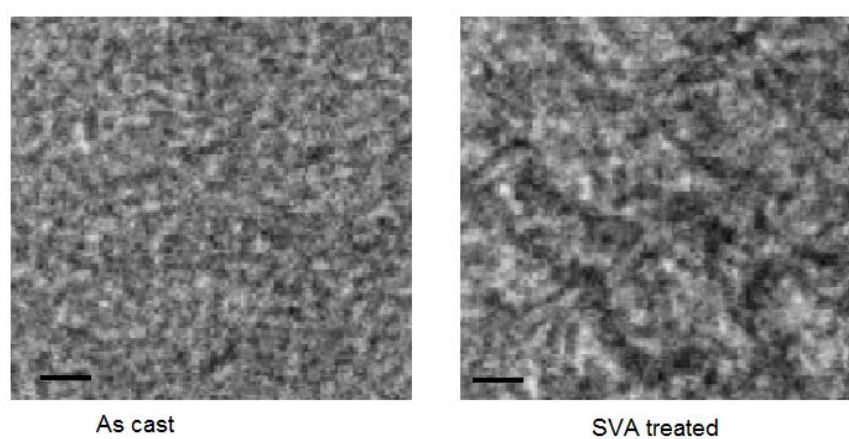


Figure S5. TEM images (scale bar 100 nm) of as cast and SVA treated LCS01:PC₇₁BM thin films

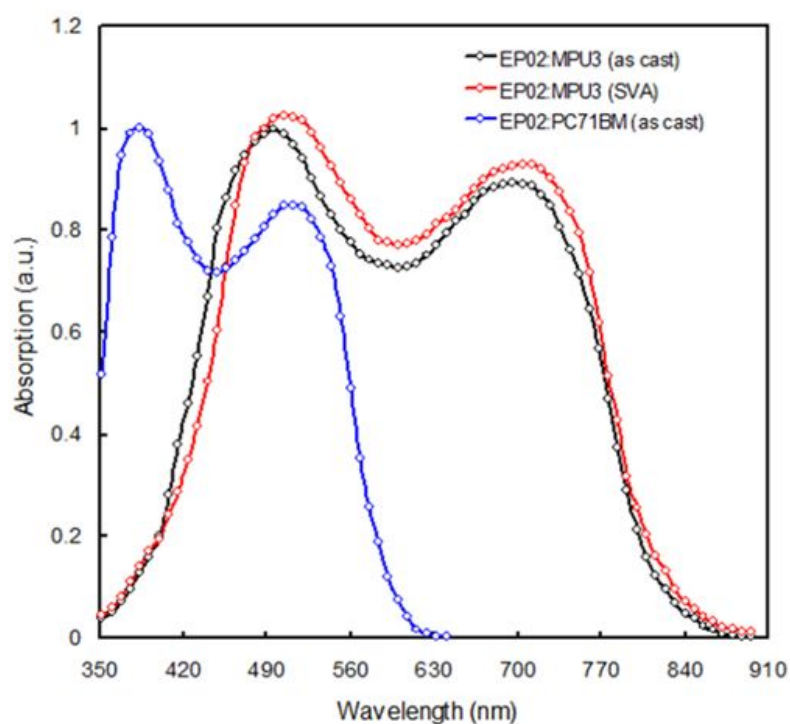


Figure S6. Normalized optical absorption spectra of EP02:MPU3 (as cast), EP02:MPU3 (SVA) and EP02:PC₇₁BM (as cast) thin films.

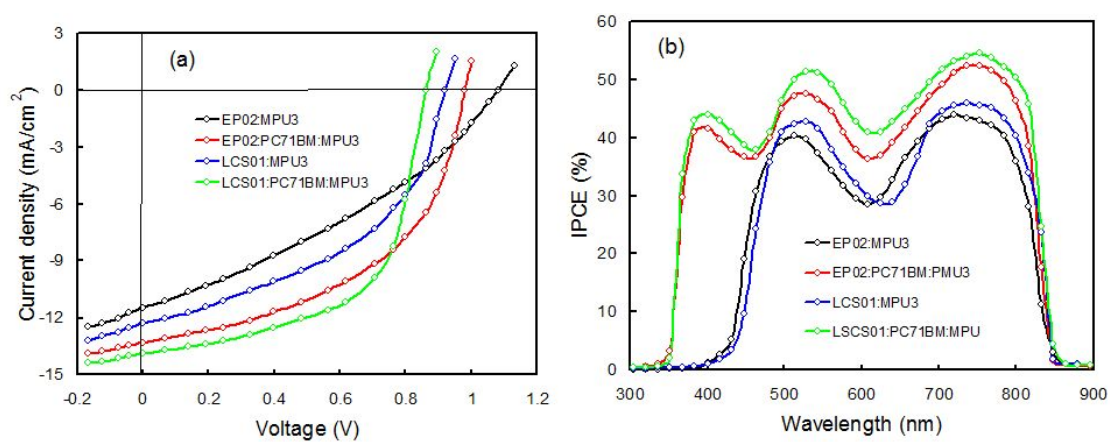


Figure S7 (a) J-V characteristics under illumination and **(b)** IPCE spectra of the OSCs based on as cast optimized binary and ternary active layers.

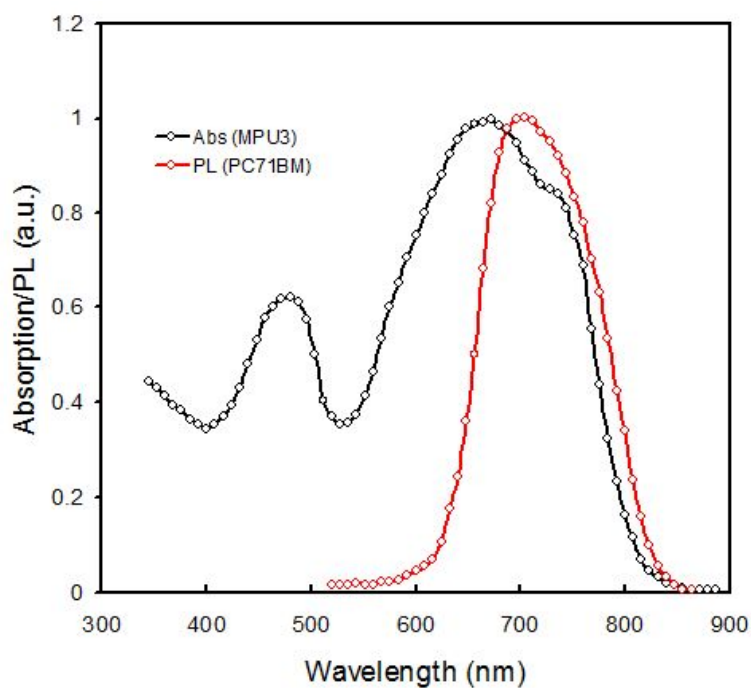


Figure S8 Absorption spectra of MPU3 thin film and PL spectra of PC₇₁BM thin film.

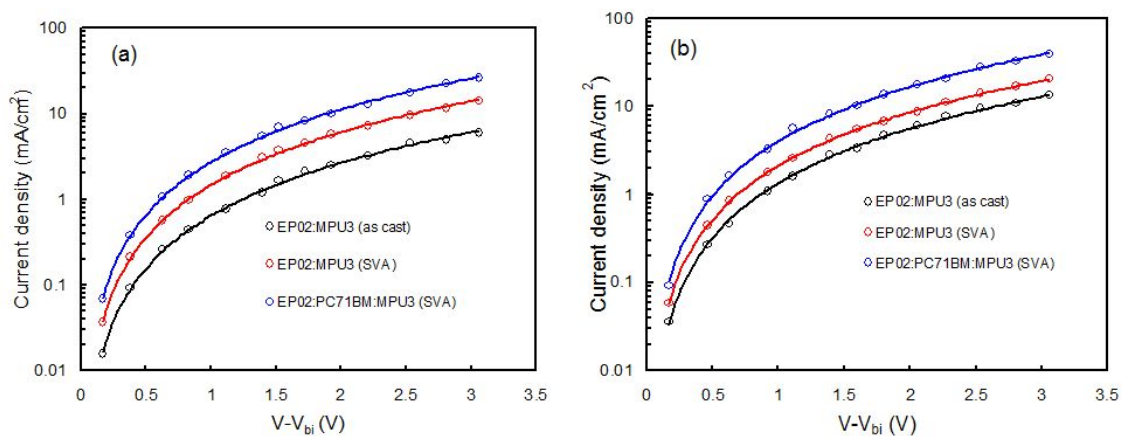


Figure S9 Dark J-V characteristics of the (a) hole and (b) electron only devices for binary and ternary based active layer processed under different conditions.

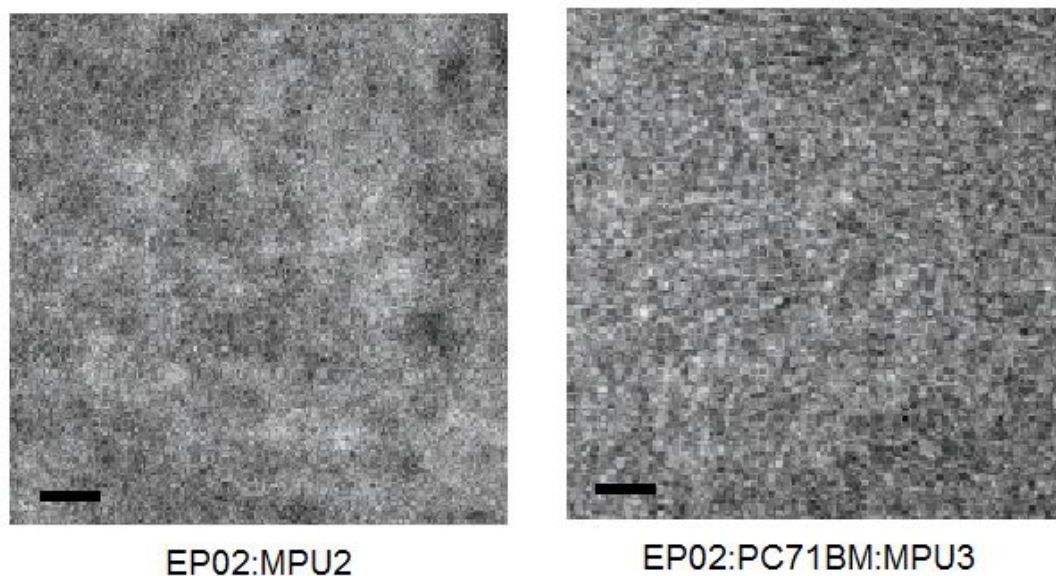


Figure S10 TEM images (scale bar 100 nm) of optimized binary EP02:MPU3 and ternary EP02:PC₇₁BM:MPU3 blended films.

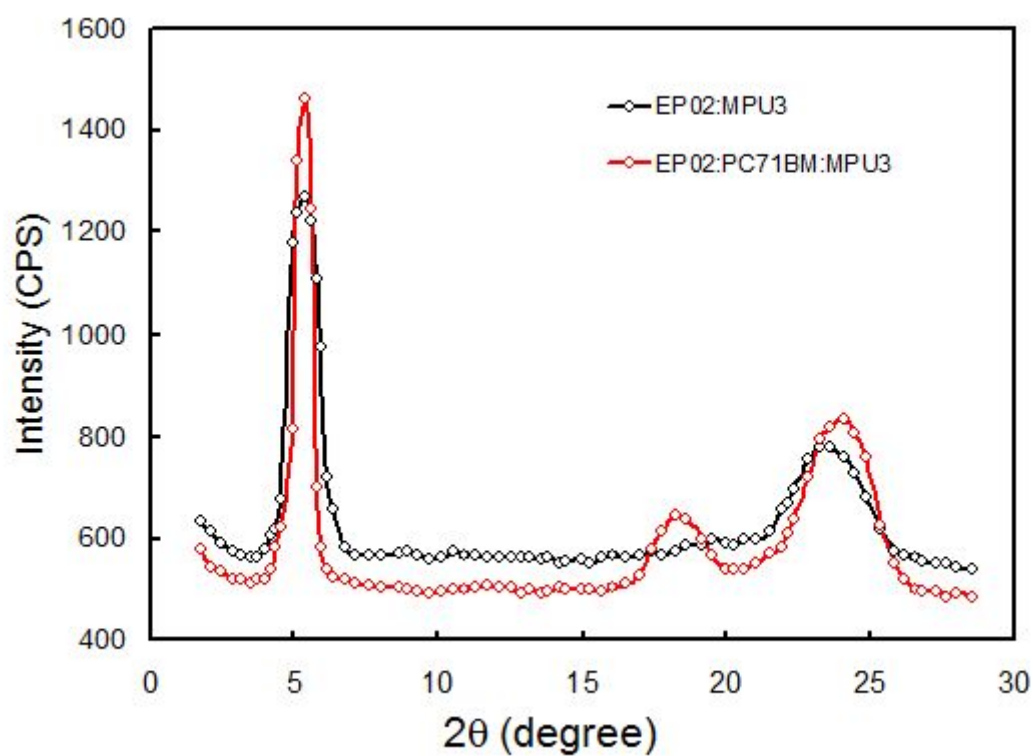


Figure S11. The XRD patterns of binary (EP02:MPU3) and ternary (EP02:PC₇₁BM:MPU3) films.

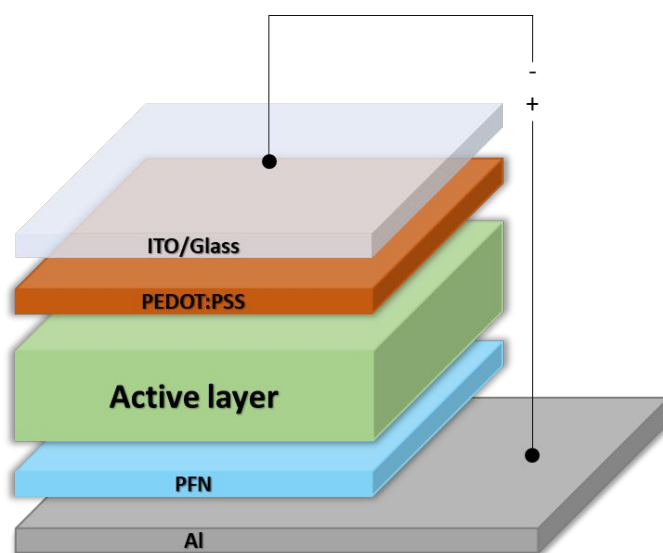


Figure S12. Device structure.